

Direct Adaptive Control of Grid-Connected Power Converters via Output-Feedback Data-Enabled Policy Optimization

Feiran Zhao, Ruohan Leng, Linbin Huang, Huanhai Xin, Keyou You, Florian Dörfler

Abstract—Power electronic converters are gradually becoming the main components of modern power systems due to the increasing integration of renewable energy sources. However, power converters may become unstable when interacting with the complex and time-varying power grid. To deal with this problem, an adaptive control design scheme for power converters is preferable, which can capture the closed-loop dynamical interaction between the converter and the grid via online data. In this paper, we propose an adaptive data-driven control method, called data-enabled policy optimization (DeePO), to stabilize power converters by using only online input-output data. Our contributions are threefold. First, we propose a covariance parameterization of partially observed linear systems with input-output data. Second, we develop a DeePO algorithm, which updates the parameterized policy with data-based gradient descent to achieve computationally efficient adaptive control. Third, we use high-fidelity simulations to verify that DeePO can effectively stabilize grid-connected power converters and quickly adapt to the changes in the power grid.

I. INTRODUCTION

Modern power systems feature a large-scale integration of power electronic converters, as they act as interfaces between the AC power grid and renewable energy sources, high-voltage DC (HVDC) systems, energy storage systems, and electric vehicles [1]. The large-scale integration of converters is fundamentally changing the power system dynamics, as they are significantly different from traditional synchronous generators (SGs). Usually, multiple nested control loops, based on fixed-parameter PI regulators, are needed in converters to achieve voltage, current, and power regulations. Under these control loops, power converters exhibit complicated interaction with the power grid and may easily tend to be unstable due to unforeseen grid conditions [2]–[4]. Such instability issues have been widely observed in practice [5], which poses challenges to the secure operation of modern power systems and impedes further integration of renewables.

The instability in converter systems is caused by the closed-loop interaction between the converter and the com-

plex power grid, which often occurs when the converter’s control strategy does not fit into the grid characteristics [6], [7]. Hence, the control design of converters should take into account the power grid dynamics for the sake of stability. However, the power grid is unknown, nonlinear, and time-varying from the perspective of a converter. Moreover, the grid structure and parameters are difficult to obtain in real time. Hence, it is nearly impossible to establish an exact dynamical model of a power grid for the control design of converters. As a remedy, engineers often use an overly simplified model for the power grid (e.g., an infinite bus) and tune the controller based on engineering experience and iterative trial-and-error approaches, which can be expensive, time-consuming, and lacking stability guarantees due to the model mismatch. While existing robust control methods can be used to handle the model mismatch [8], [9], they usually lead to conservative controllers when large changes appear in the power grid (e.g., tripping of transmission lines or even HVDC stations). Ideally, the controller of converters should be *adaptive*, i.e., it is able to perceive and quickly adapt to changes in the power grid by using online data.

Recently, there has been a renewed interest in *direct* data-driven control, which bypasses the system identification (SysID) step and learns the controller directly from a batch of persistently exciting data [10]–[19]. This approach is end-to-end, easy to implement, and has seen many successful applications [20]–[22]. Following this line, our previous work proposes a direct data-driven linear quadratic regulator (LQR) method [23], [24]. It is adaptive in the sense that the control performance is improved in real time by using online closed-loop data. We call this method **Data-enabled Policy Optimization (DeePO)**, where the policy is parameterized with sample covariance of input-state data and updated using gradient methods. DeePO has a recursive algorithmic implementation and hence is computationally efficient. From a theoretical perspective, it meets provable stability and convergence guarantees for linear time-invariant systems. All these key features render DeePO an ideal data-driven control method for power converters.

In this paper, we propose a DeePO method to mitigate oscillations in power converter systems. Since the power converter system is only partially observed, i.e., the full state is unmeasurable, we first extend the covariance parameterization of the system with input-state data in [23], [24] to that with input-output data. This is achieved by regarding a finite length of past input-output trajectory as the state and using the corresponding covariance to parameterize the closed-loop system. Then, we propose the DeePO algorithm for

F. Zhao is with the Department of Automation and BNRist, Tsinghua University, Beijing 100084, China, and the Department of Information Technology and Electrical Engineering, ETH Zurich, 8092 Zurich, Switzerland. (e-mail: zhaofe@control.ee.ethz.ch)

R. Leng, L. Huang, and H. Xin are with the College of Electrical Engineering at Zhejiang University, Hangzhou 310027, China. (email: lengruohan@zju.edu.cn, hlinbin@zju.edu.cn, xinhh@zju.edu.cn)

K. You is with the Department of Automation and BNRist, Tsinghua University, Beijing 100084, China. (e-mail: youky@tsinghua.edu.cn.)

F. Dörfler is with the Department of Information Technology and Electrical Engineering, ETH Zurich, 8092 Zurich, Switzerland. (e-mail: dorfler@ethz.ch)

direct adaptive control of partially observed systems. Finally, we apply the DeePO algorithm to stabilize power converter and direct-drive wind generator systems, both of which are unknown, state-unmeasurable, and encounter sudden change of dynamics due to grid changes. Simulation results show that DeePO enables efficient online adaptation and effectively prevents instabilities in grid-connected power converters. Compared with our previous works applying data-enabled predictive control (DeePC) to power converters [21], [25], DeePO offers a significantly reduced online computational burden, making it more suitable for scenarios where the processor cannot solve a quadratic program in real time.

The rest of the paper is organized as follows. Section II formulates the stabilization problem of power converter systems. Section III introduces the adaptive LQR control and the DeePO method. Section IV extends the DeePO algorithm to input-output systems. Section V performs simulations on the converter systems. Conclusion is made in Section VI.

Notation. We use I_n to denote the n -by- n identity matrix. We use $\rho(\cdot)$ to denote the spectral radius of a square matrix. We use A^\dagger to denote the pseudoinverse of a matrix A . We use $(S)_i$ to denote the i -th column of a block matrix S .

II. STABILIZATION OF GRID-CONNECTED POWER CONVERTERS

In this section, we introduce the stabilization problem of DC-AC power converter systems, taking into account both the DC-side and AC-side dynamics. Notice that power converters are widely used as the interface between the AC power grid and a DC source, such as lithium battery-based energy storage systems or direct-drive wind generators. The lithium batteries generate a constant DC voltage, and the converter aims to regulate the active and reactive power, as shown in Fig. 1. By comparison, when used as the grid interface of direct-drive wind generators, the converter needs to regulate the DC voltage and the reactive power, as will be shown in Section V. In both cases, the converter plays an important role in maintaining stable and reliable power transfer between the DC side and the AC side.

A. Power converter systems

Consider the grid-connected power converter system in Fig. 1, which has a phase-locked loop (PLL), power/current control loops, and (abc/dq) coordinate transformation blocks [6]. Due to proprietary manufacturer models and the complexity of the power grid, the power converter together with the grid is a black-box system for the subsequent stabilization control design. While inherently nonlinear, the system can be linearized around its equilibrium point for analysis. Note that the time-varying nature of the power grid may induce a time-varying operating point. Without loss of generality, consider the state-space model linearized at the origin

$$\begin{aligned} x_{t+1} &= Ax_t + Bu_t + w_t, \\ y_t &= Cx_t + v_t, \end{aligned} \quad (1)$$

where $x_t \in \mathbb{R}^n$ is the state variable (could be unmeasurable, e.g., variables in the power grid side), $u_t \in \mathbb{R}^m$ is the

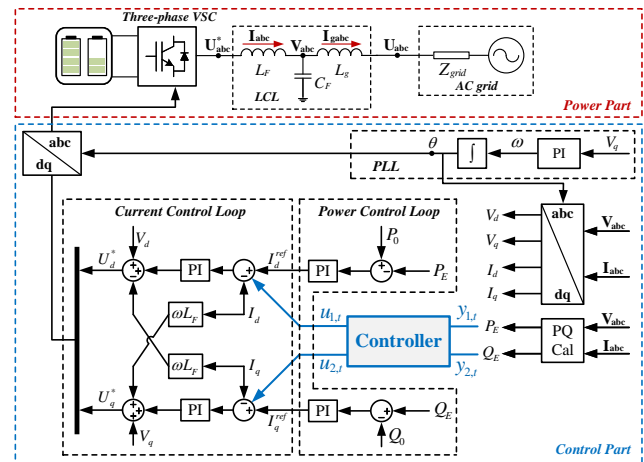


Fig. 1. One-line diagram of a grid-connected power converter. Here the DC side is connected to lithium batteries, while it can also be wind turbines.

control input (e.g., additional signals added to the current references; see Fig. 1), $y_t \in \mathbb{R}^d$ is the output (e.g., active and reactive power in our setting), w_t is the process noise, and v_t is the measurement noise. The unknown system (A, B, C) is controllable and observable, but it may be subject to sudden impedance changes due to external grid changes, e.g., changes of Z_{grid} in Fig. 1. Such events may lead to poorly damped or even unstable oscillations.

Our objective is to find a policy as feedback of the past input-output trajectory $u_t = \pi_t(u_{-\infty}, y_{-\infty}, \dots, u_{t-1}, y_{t-1})$ so that the output is regulated to zero with low control effort.

B. Challenges in stabilization of power converter systems (DC source + DC-AC converter + AC power grid)

There are three main challenges in the stabilization of power converter systems:

- **unknown model:** Power converter systems often exhibit high-order characteristics, rendering it difficult to establish exact dynamical models. Specifically, the exact dynamics of the DC source and the converter are usually hard to obtain (and therefore unknown) due to proprietary manufacturer models and their complexity, e.g., the complex mechanical behaviors of wind turbines. Moreover, the power grid is also unknown when designing a controller for the converter, as the grid is large-scale and time-varying (therefore hard to model).
- **measurement limitations:** Internal states are not measurable and hence we can only use input-output information for the control design.
- **sudden change of dynamics:** Variations in grid conditions, operating states of power converters, and control parameter adjustments cause the power converter system to encounter sudden changes in dynamics [21].

C. Our approach

In this paper, we propose a direct data-driven method to solve the stabilization problem of power converter systems without SysID. Our approach is based on data-enabled policy optimization (DeePO), an adaptive linear quadratic control

method introduced in our recent work [23], [24]. It is data-driven and does not involve any explicit SysID. Moreover, DeePO uses online closed-loop data to adaptively update the control policy, making it an ideal method to deal with time-varying dynamics.

In the sequel, we first recapitulate the DeePO method with input-state data in [23], [24]. Then, we extend DeePO to the input-output setting. Finally, we discuss its implementation on power converter systems and perform simulations to validate the effectiveness of DeePO.

III. DIRECT ADAPTIVE LQR CONTROL VIA DATA-ENABLED POLICY OPTIMIZATION

In this section, we first introduce the linear quadratic regulator (LQR). Then, we recapitulate data-enabled policy optimization for adaptive learning of the LQR [23], [24].

A. The linear quadratic regulator

Consider a linear time-invariant system with fully measurable state

$$\begin{cases} x_{t+1} = Ax_t + Bu_t + w_t \\ h_t = \begin{bmatrix} Q^{1/2} & 0 \\ 0 & R^{1/2} \end{bmatrix} \begin{bmatrix} x_t \\ u_t \end{bmatrix} \end{cases} \quad (2)$$

Here, h_t is the performance signal of interest, (A, B) is controllable, and the weighting matrices (Q, R) are positive definite.

The LQR problem is phrased as finding a state-feedback gain $K \in \mathbb{R}^{m \times n}$ that minimizes the \mathcal{H}_2 -norm of the transfer function $\mathcal{T}(K) : w \rightarrow h$ of the closed-loop system

$$\begin{bmatrix} x_{t+1} \\ h_t \end{bmatrix} = \begin{bmatrix} A + BK & I_n \\ \begin{bmatrix} Q^{1/2} \\ R^{1/2} \end{bmatrix} & 0 \end{bmatrix} \begin{bmatrix} x_t \\ w_t \end{bmatrix}.$$

When $A + BK$ is stable, it holds that [26]

$$\|\mathcal{T}(K)\|_2^2 = \text{Tr}((Q + K^\top RK)\Sigma_K) =: C(K), \quad (3)$$

where Σ_K is the closed-loop state covariance matrix obtained as the positive definite solution to the Lyapunov equation

$$\Sigma_K = I_n + (A + BK)\Sigma_K(A + BK)^\top. \quad (4)$$

We refer to $C(K)$ as the LQR cost and to (3)-(4) as a *policy parameterization* of the LQR.

It is well-known that the optimal LQR gain K^* is unique and can be found by, e.g., solving an algebraic Riccati equation with (A, B) [26]. When (A, B) is unknown, data-driven methods learn the LQR gain from input-state data. In the sequel, we recall the DeePO approach proposed in our previous work [23], [24].

B. DeePO for direct adaptive LQR control

Policy optimization (PO) refers to a class of direct design methods, where the policy is parameterized and recursively updated using gradient methods [27]. In particular, DeePO uses the sample covariance of input-state data to parameterize

the policy [24]. Consider the t -long time series of states, inputs, noises, and successor states

$$\begin{aligned} X_{0,t} &:= [x_0 \ x_1 \ \dots \ x_{t-1}] \in \mathbb{R}^{n \times t}, \\ U_{0,t} &:= [u_0 \ u_1 \ \dots \ u_{t-1}] \in \mathbb{R}^{m \times t}, \\ W_{0,t} &:= [w_0 \ w_1 \ \dots \ w_{t-1}] \in \mathbb{R}^{n \times t}, \\ X_{1,t} &:= [x_1 \ x_2 \ \dots \ x_t] \in \mathbb{R}^{n \times t}, \end{aligned}$$

which satisfy the system dynamics

$$X_{1,t} = AX_{0,t} + BU_{0,t} + W_{0,t}. \quad (5)$$

Assuming that the data is *persistently exciting (PE)* [28], i.e., the block matrix of input and state data $D_{0,t} := [U_{0,t}^\top, X_{0,t}^\top]^\top$ has full row rank

$$\text{rank}(D_{0,t}) = m + n, \quad (6)$$

the *covariance parameterization* [24] of K is given by

$$\begin{bmatrix} K \\ I_n \end{bmatrix} = \frac{1}{t} D_{0,t} D_{0,t}^\top V =: \Phi_t V, \quad (7)$$

where $\Phi_t \succ 0$ denotes the sample covariance of input-state data, and $V \in \mathbb{R}^{(n+m) \times n}$ is the parameterized policy.

With the covariance parameterization (7), the LQR problem (3)-(4) can be expressed by raw data matrices $(X_{0,t}, U_{0,t}, X_{1,t})$ and the optimization matrix V . For brevity, let $\bar{X}_{0,t} = X_{0,t} D_{0,t}^\top / t$ and $\bar{U}_{0,t} = U_{0,t} D_{0,t}^\top / t$ be a partition of Φ_t , and let $\bar{W}_{0,t} = W_{0,t} D_{0,t}^\top / t$ be the noise-state-input covariance, and finally define the covariance with respect to the successor state $\bar{X}_{1,t} = X_{1,t} D_{0,t}^\top / t$. Note that the dimension of the covariance matrices does not depend on t . Then, the closed-loop matrix can be written as

$$A + BK = [B, A] \begin{bmatrix} K \\ I_n \end{bmatrix} \stackrel{(7)}{=} [B, A] \Phi_t V \stackrel{(5)}{=} (\bar{X}_{1,t} - \bar{W}_{0,t}) V.$$

Following the certainty-equivalence principle [14], we disregard the unmeasurable $\bar{W}_{0,t}$ and use $\bar{X}_{1,t} V$ as the closed-loop matrix. After substituting $A + BK$ with $\bar{X}_{1,t} V$ in (3)-(4) and leveraging (7), the LQR problem becomes

$$\begin{aligned} &\underset{V}{\text{minimize}} \quad J_t(V) := \text{Tr} \left((Q + V^\top \bar{U}_{0,t}^\top R \bar{U}_{0,t} V) \Sigma_t(V) \right), \\ &\text{subject to} \quad \bar{X}_{0,t} V = I_n, \end{aligned} \quad (8)$$

where $\Sigma_t(V) = I_n + \bar{X}_{1,t} V \Sigma_t(V) V^\top \bar{X}_{1,t}^\top$ is a covariance parameterization of (4), and the gain matrix can be recovered by $K = \bar{U}_{0,t} V$. We refer to (8) as the direct data-driven LQR problem, which does not involve any explicit SysID.

The DeePO algorithm uses online gradient descent of (8) to recursively update V . The details are presented in Algorithm 1, which alternates between control (line 2) and policy update (line 3-5). The initial stabilizing policy can be either user-specified or computed by solving (8) with offline data. At time t , we apply the linear state feedback policy $u_t = K_t x_t + e_t$ for control, where e_t is a probing noise used to ensure the PE rank condition (6). We use online projected gradient descent in (10) to update the parameterized policy, where the projection $\Pi_{\bar{X}_{0,t+1}} := I_{n+m} - \bar{X}_{0,t+1}^\dagger \bar{X}_{0,t+1}$

onto the nullspace of $\bar{X}_{0,t+1}$ is to ensure the subspace constraint in (8). The gradient can be computed by the following lemma. Define the feasible set of (8) (i.e., the set with stable closed-loop matrices) as $\mathcal{S}_t := \{V \mid \bar{X}_{0,t}V = I_n, \rho(\bar{X}_{1,t}V) < 1\}$.

Lemma 1 ([24]): For $V \in \mathcal{S}_t$, the gradient of $J_t(V)$ with respect to V is given by

$$\nabla J_t(V) = 2 \left(\bar{U}_{0,t}^\top R \bar{U}_{0,t} + \bar{X}_{1,t}^\top P_t \bar{X}_{1,t} \right) V \Sigma_t(V), \quad (9)$$

where P_t satisfies the Lyapunov equation

$$P_t = Q + V^\top \bar{U}_{0,t}^\top R \bar{U}_{0,t} V + V^\top \bar{X}_{1,t}^\top P_t \bar{X}_{1,t} V.$$

DeePO is *direct and adaptive* in the sense that it directly uses online closed-loop data to update the policy. Thus, it can rapidly adapt to dynamic changes reflected in the data. Algorithm 1 has a recursive policy update and can be implemented efficiently. Specifically, all covariance matrices and the inverse Φ_{t+1}^{-1} have recursive updates. Moreover, the parameterization can be updated recursively via rank-one update, i.e.,

$$V_{t+1} = \frac{t+1}{t} \left(V_t' - \frac{\Phi_t^{-1} \phi_t \phi_t^\top V_t'}{t + \phi_t^\top \Phi_t^{-1} \phi_t} \right),$$

where $\phi_t = [u_t^\top, x_t^\top]^\top$, and Φ_t^{-1} and V_t' are given from the last iteration. Theoretically, it is shown that under mild assumptions the policy $\{K_t\}$ converges to the optimal LQR gain. We refer to [24, Section IV] for detailed discussions.

The DeePO framework developed so far considers the state feedback setting. However, the state of power converter system (1) is not measurable, and only input-output data is available for control design. Such a system is typically referred to as partially observed [29]. Next, we extend DeePO to partially observed systems for adaptive control using input-output data.

Algorithm 1 DeePO for direct adaptive LQR control

Input: Offline data $(X_{0,t_0}, U_{0,t_0}, X_{1,t_0})$, an initial policy K_{t_0} , and a stepsize η .

- 1: **for** $t = t_0, t_0 + 1, \dots$ **do**
- 2: Apply $u_t = K_t x_t + e_t$ and observe x_{t+1} .
- 3: Update covariance matrices Φ_{t+1} and $\bar{X}_{1,t+1}$.
- 4: **Policy parameterization:** given K_t , solve V_{t+1} via

$$V_{t+1} = \Phi_{t+1}^{-1} \begin{bmatrix} K_t \\ I_n \end{bmatrix}.$$

- 5: **Update of the parameterized policy:** perform one-step projected gradient descent

$$V'_{t+1} = V_{t+1} - \eta \Pi_{\bar{X}_{0,t+1}} \nabla J_{t+1}(V_{t+1}), \quad (10)$$

where the gradient $\nabla J_{t+1}(V_{t+1})$ is given by Lemma 1.

- 6: **Gain update:** update the control gain by

$$K_{t+1} = \bar{U}_{0,t+1} V'_{t+1}.$$

- 7: **end for**
-

IV. OUTPUT-FEEDBACK DEEPO FOR PARTIALLY OBSERVED SYSTEMS

In this section, we extend DeePO for direct adaptive control of partially observed systems using input-output data.

Consider the system (1). Since the state is unmeasurable, we represent (1) with a non-minimal realization using input and output signals. Denote the input trajectory, the output trajectory, and their stack from time $t-n$ to $t-1$ as

$$u_{t,n} = \begin{bmatrix} u_{t-1} \\ \vdots \\ u_{t-n} \end{bmatrix}, \quad y_{t,n} = \begin{bmatrix} y_{t-1} \\ \vdots \\ y_{t-n} \end{bmatrix}, \quad z_t = \begin{bmatrix} u_{t,n} \\ y_{t,n} \end{bmatrix}$$

respectively. Define the observability matrix

$$\mathcal{O} = \begin{bmatrix} CA^{n-1} \\ \vdots \\ CA \\ C \end{bmatrix},$$

the controllability matrices $\mathcal{C} = [B \ AB \ \dots \ A^{n-1}B]$, $\mathcal{C}_w = [I \ A \ \dots \ A^{n-1}]$, and the Toeplitz matrices capturing the impulse and disturbance response

$$\mathcal{T} = \begin{bmatrix} 0 & CB & CAB & \dots & CA^{n-2}B \\ 0 & 0 & CB & \dots & CA^{n-3}B \\ \vdots & \vdots & \ddots & \ddots & \vdots \\ 0 & \dots & 0 & 0 & CB \\ 0 & 0 & 0 & 0 & 0 \end{bmatrix},$$

$$\mathcal{T}_w = \begin{bmatrix} 0 & C & CA & \dots & CA^{n-2} \\ 0 & 0 & C & \dots & CA^{n-3} \\ \vdots & \vdots & \ddots & \ddots & \vdots \\ 0 & \dots & 0 & 0 & C \\ 0 & 0 & 0 & 0 & 0 \end{bmatrix}.$$

Let $S = [C(\mathcal{C} - A^n \mathcal{O}^\dagger \mathcal{T}), CA^n \mathcal{O}^\dagger]$, $d_t = C(\mathcal{C}_w - A^n \mathcal{O}^\dagger \mathcal{T}_w)w_{t,n} - CA^n \mathcal{O}^\dagger v_{t,n} + v_t$. Then, we have the following results, the proof of which is provided in the appendix.

Theorem 1 (Non-minimal controllable realization): A non-minimal controllable realization of (1) is given by (11) shown at the bottom of the next page.

Remark 1: The length of the past trajectory used to represent the state does not necessarily match the system order n . In fact, it only needs to exceed the system lag (i.e., the observability index), under which the dimension of z_t can be reduced. ■

Then, we can apply DeePO for the system (11), whose state is measurable. Define the matrix of input-output data

$$Z_{0,t} = [z_0 \ z_1 \ \dots \ z_{t-1}] \in \mathbb{R}^{n(m+d) \times t}.$$

Assume that the data is PE, i.e., the block matrix $[U_{0,t}^\top, Z_{0,t}^\top]^\top$ has full row rank. Then, the covariance parameterization of K for the system (11) is given by

$$\begin{bmatrix} K \\ I_{n(m+d)} \end{bmatrix} = \frac{1}{t} \begin{bmatrix} U_{0,t} \\ Z_{0,t} \end{bmatrix} \begin{bmatrix} U_{0,t} \\ Z_{0,t} \end{bmatrix}^\top V =: \Psi_t V,$$

where $V \in \mathbb{R}^{n(2m+d) \times n(m+d)}$.

Define the sample covariance matrices

$$\bar{Z}_{0,t} = \frac{1}{t} Z_{0,t} \begin{bmatrix} U_{0,t} \\ Z_{0,t} \end{bmatrix}^\top, \quad \bar{Z}_{1,t} = \frac{1}{t} Z_{1,t} \begin{bmatrix} U_{0,t} \\ Z_{0,t} \end{bmatrix}^\top.$$

Denote the realization (11) as (A_z, B_z, C_z) . Following the certainty-equivalence principle and disregarding d_t , we approximate the closed-loop matrix by

$$A_z + B_z K \approx \bar{Z}_{1,t} V.$$

Then, the LQR problem of (11) is parameterized as

$$\begin{aligned} & \underset{V}{\text{minimize}} \quad J_t(V) := \text{Tr} \left((Q_1 + V^\top \bar{U}_{0,t}^\top R_z \bar{U}_{0,t} V) \Sigma_t(V) \right), \\ & \text{subject to} \quad \bar{Z}_{0,t} V = I_n, \end{aligned} \quad (12)$$

where Q_z, R_z are positive definite matrices with proper dimensions, $\Sigma_t(V) = I_n + \bar{Z}_{1,t} V \Sigma_t(V) V^\top \bar{Z}_{1,t}^\top$, and the gain matrix can be recovered by $K = \bar{U}_{0,t} V$.

The DeePO method for partially observed systems is provided in Algorithm 2. Next, we apply Algorithm 2 to stabilize power converter and renewable energy systems.

Algorithm 2 DeePO for partially observed systems

Input: Offline data $(Z_{0,t_0}, U_{0,t_0}, Z_{1,t_0})$, an initial policy K_{t_0} , and a stepsize η .

- 1: **for** $t = t_0, t_0 + 1, \dots$ **do**
- 2: Apply $u_t = K_t z_t + e_t$ and observe z_{t+1} .
- 3: Update covariance matrices Φ_{t+1} and $\bar{Z}_{1,t+1}$.
- 4: **Policy parameterization:** given K_t , solve V_{t+1} via

$$V_{t+1} = \Psi_{t+1}^{-1} \begin{bmatrix} K_t \\ I_n \end{bmatrix}.$$

- 5: **Update of the parameterized policy:** perform one-step projected gradient descent

$$V'_{t+1} = V_{t+1} - \eta \Pi_{\bar{Z}_{0,t+1}} \nabla J_{t+1}(V_{t+1}).$$

- 6: **Gain update:** update the control gain by

$$K_{t+1} = \bar{U}_{0,t+1} V'_{t+1}.$$

- 7: **end for**
-

V. DEEPO FOR STABILIZATION OF POWER CONVERTERS AND RENEWABLE ENERGY SYSTEMS

In this section, we first discuss the implementation of DeePO on the power converter systems. Then, we perform simulations for a grid-connected power converter and a direct-drive wind generator.

A. Implementation of DeePO for power converter systems

We consider two typical power converter systems: a grid-connected power converter (with lithium batteries as the DC source) in Fig. 1 and a direct-drive (type 4) wind generator in Fig. 3, which also uses a converter as the grid interface. Both systems share similar control challenges, including unknown models, measurement limitations, and potential change of dynamics. While Algorithm 2 considers only time-invariant systems, it can potentially handle changes in the system dynamics. This is because DeePO uses online closed-loop data to update the policy in real time and can quickly adapt to changes. Moreover, since Algorithm 2 has a recursive implementation, the online update of the policy is computationally efficient.

For both systems, we select the deviations of active and reactive power from their reference values as the outputs of the unknown system, denoted by $y = [P_E - P_0, Q_E - Q_0]^\top$. The DeePO method is configured to provide two control inputs that are added to the current references of the system. All input and output signals are expressed in per-unit (p.u.) values. Since directly measuring internal state variables is challenging, we construct new state variables using input-output information as $z_t = [u_{t,T_{\text{ini}}}, y_{t,T_{\text{ini}}}]^\top$, where the length of the initial trajectory for constructing new states is set to $T_{\text{ini}} = 6$ for both systems.

The parameters for the two systems are set as follows:

- **sampling frequency:** The sampling frequency is chosen as 200 Hz.
- **trajectory length T :** The trajectory length is set to 300 for the power converter and 600 for the wind generator to satisfy the persistency of excitation condition.
- **weighting matrices:** The input weighting matrix is set as $R = I_m$, while the output weighting matrix is set as $Q = \text{diag}(I_{mT_{\text{ini}}}, 100I_{pT_{\text{ini}}})$.

$$z_{t+1} = \begin{bmatrix} 0 & 0 & \cdots & 0 & 0 & 0 & 0 & \cdots & 0 & 0 \\ I_m & 0 & \cdots & 0 & 0 & 0 & 0 & \cdots & 0 & 0 \\ 0 & I_m & \cdots & 0 & 0 & 0 & 0 & \cdots & 0 & 0 \\ \vdots & \vdots & \ddots & \vdots & \vdots & \vdots & \vdots & \ddots & \vdots & \vdots \\ 0 & 0 & \cdots & I_m & 0 & 0 & 0 & \cdots & 0 & 0 \end{bmatrix} z_t + \begin{bmatrix} I_m \\ 0 \\ 0 \\ \vdots \\ 0 \end{bmatrix} u_t + \begin{bmatrix} 0 \\ 0 \\ 0 \\ \vdots \\ I_d \\ 0 \end{bmatrix} d_t \quad (11)$$

$$y_t = S z_t + d_t$$

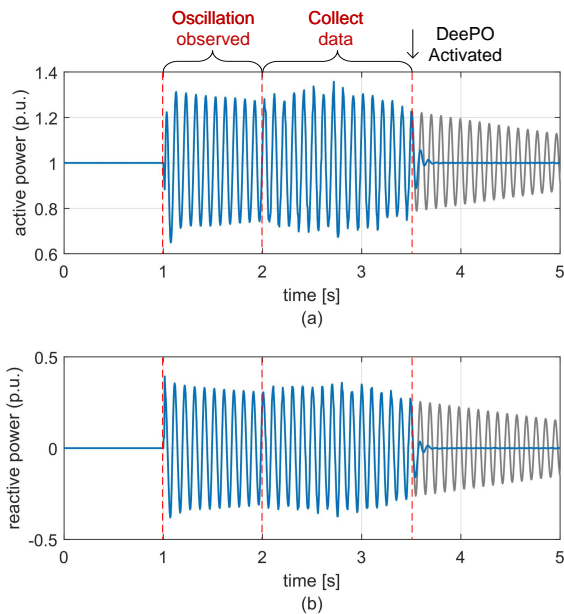


Fig. 2. Time-domain responses of the grid-connected power converter. The DeePO is activated at $t = 3.5$ s. — with DeePO; — without DeePO.

- **gradient descent parameters:** The stepsize for gradient descent is set as $\eta = 0.005$. For the grid-connected power converter, the number of gradient descent steps per control sampling time is set to 1. For the wind generator, two configurations are compared with 1 and 10 gradient descent steps per control sampling time.

B. Simulations on a grid-connected power converter

The grid-connected power converter system considered in this study is shown in Fig. 1, where we employ the DeePO controller. The objective of the DeePO controller is to regulate the deviations of active and reactive power from their references to zero with minimal control effort, thereby effectively mitigating power oscillations caused by grid disturbances.

Fig. 2 shows the time-domain responses of the power converter. At $t = 1.0$ s, we change the short circuit ratio of the system from 5 to 2.21 to emulate an event in the power grid, for example, tripping of transmission lines. It can be seen that the converter starts to oscillate after the disturbance, which is caused by the interactions among PLL, current/power control loops, and the weak power grid [2]. Such oscillations are undesirable, as they may trigger resonance in the system, increase the risk of equipment failure, and even result in grid collapse.

After the oscillation is observed, we inject band-limited white noise signals into the system through the two input channels from $t = 2.0$ s to $t = 3.5$ s to excite the system and collect data. The DeePO controller is activated at $t = 3.5$ s, providing real-time control inputs that effectively counteract the oscillation. As depicted in Fig. 2, DeePO effectively damps the oscillation and restores the stable operation of the power converter. In contrast, the responses of the power converter without DeePO are shown as the grey lines in

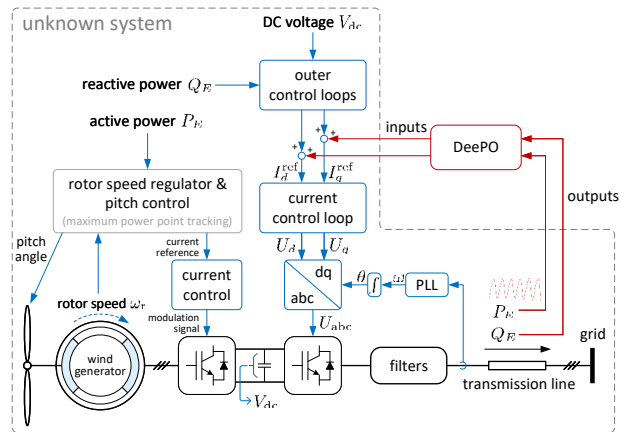


Fig. 3. The application of DeePO to stabilize a direct-drive wind generator.

Fig. 2, where the system exhibits sustained active and reactive power oscillations, indicating a low stability margin and increasing the risk of equipment damage and potential cascading failures in the power system.

C. Simulations on a direct-drive wind generator

We consider now a direct-drive wind generator with a high-fidelity model implemented in MATLAB/Simulink (2023b) [21]. The wind generator model here is more complicated than the converter model in the last subsection, as it not only has a converter as the grid interface, but also considers the generator dynamics on the DC side. The simulation model includes detailed turbine dynamics, flux dynamics, filters, speed control, pitch control, converter control, and maximum power point tracking (MPPT). The grid is modeled as a voltage source behind a transmission line with unknown impedance, which impacts the wind generator in a closed-loop manner. The whole system is illustrated in Fig. 3. Due to proprietary manufacturer models and the complexity of the power grid, its exact dynamical model can hardly be derived or identified. In what follows, we apply the DeePO method in Algorithm 2 to stabilize the wind generator.

Fig. 4 shows the time-domain responses of the wind generator under different configurations of DeePO. At $t = 1.0$ s, the short circuit ratio is changed from 2.23 to 2, simulating a grid event, such as the tripping of transmission lines. Following the disturbance, the wind generator begins to oscillate.

Then, we inject band-limited white noise to collect input-output trajectory data from $t = 3.0$ s to $t = 6.0$ s. At $t = 6.0$ s, DeePO is activated and successfully provides real-time control inputs, eliminating the oscillations in both configurations, as shown in Fig. 4. In the configuration with fewer gradient descent steps per control cycle (blue line), the convergence of active and reactive power is slower, with acceptable stabilization performance. By comparison, using 10 steps (orange line) enables faster damping of oscillations. This illustrates a trade-off between computational efficiency and control performance: increasing the gradient steps improves convergence but requires higher computational effort. By comparison, the wind generator system exhibits a low

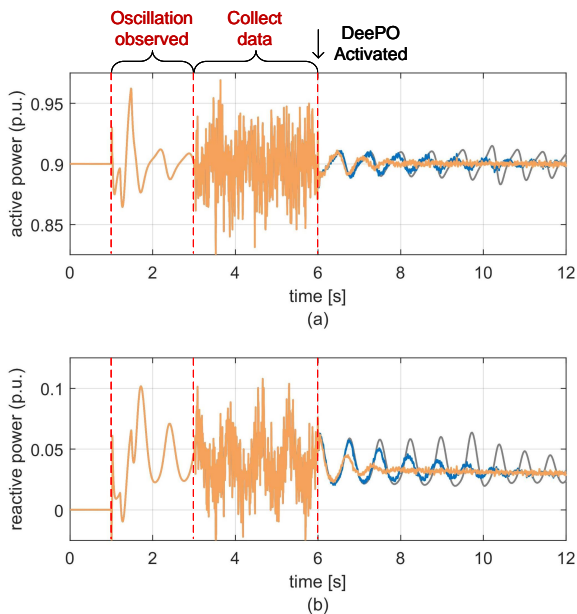


Fig. 4. The time-domain responses of the wind generator: (a) active power and (b) reactive power. The DeePO is activated at $t = 6.0$ s. — with DeePO (1 gradient descent step per control cycle); — with DeePO (10 gradient descent steps per control cycle); — without DeePO.

stability margin without DeePO (grey line in Fig. 4), with persistent oscillations in active and reactive power after $t = 6.0$ s. These persistent oscillations endanger the wind generator itself (as mechanical resonance may be triggered) and also the secure operation of power systems. We observe that the damping performance of DeePO is similar to the performance of DeePC (c.f. Fig. 14 in [21]), but the computational burden is significantly less (since DeePC requires solving a quadratic program online).

In time-varying environments, non-adaptive controllers that rely solely on historical data may fail to maintain effective control. In contrast, DeePO adapts by continuously learning from real-time data, allowing it to better accommodate time-varying system conditions. Fig. 5 shows the time-domain responses of the wind generator using a non-adaptive controller (a fixed controller that achieves similar performance to DeePO before $t = 9.0$ s) and the DeePO controller, respectively, under parameter changes and disturbances. Before $t = 9.0$ s, both controllers have converged to their respective optimal gains based on previously collected data. At $t = 9.0$ s, the DC voltage control parameters are intentionally reduced to 0.9 times of their original values, simulating a sudden change in the wind generator system. While this change does not affect the equilibrium point, it modifies the dynamic characteristics of the system. From $t = 9.0$ s to $t = 21.0$ s, the DeePO controller continues to update its control strategy by leveraging real-time data, whereas the non-adaptive controller retains its original control settings without adaptation. To ensure that the collected data are informative to update the DeePO controller, noise injection is increased between $t = 10.0$ s and $t = 17.0$ s to better excite the system and capture its dynamic characteristics.

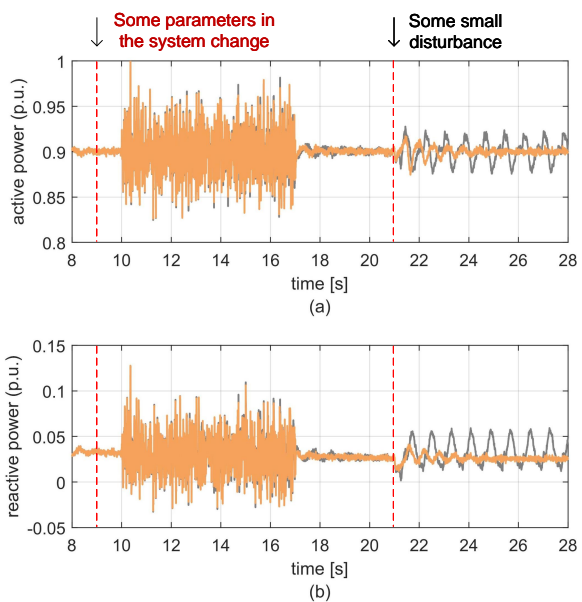


Fig. 5. The time-domain responses of the wind generator: (a) active power and (b) reactive power. — with DeePO controller; — with non-adaptive controller.

At $t = 21.0$ s, a small disturbance is introduced by injecting a q -axis voltage perturbation into the PLL. As shown in Fig. 5, the DeePO controller quickly damps out oscillations, demonstrating significantly better response performance compared to the non-adaptive controller. This improvement can be attributed to the real-time adaptation of the control policy in DeePO, which enables it to perceive changes in system dynamics and maintain superior performance under disturbances.

VI. CONCLUSION

In this paper, we proposed a data-enabled policy optimization (DeePO) method, which is direct data-driven, adaptive, based on online input-output data, and recursive in terms of implementation. We demonstrated via simulations the effectiveness of DeePO in stabilizing and mitigating undesired oscillations in a grid-connected power converter and a direct-drive wind generator. In particular, we observed that DeePO has satisfactory performance in stabilization, and shows a similar damping ratio to data-enabled predictive control (DeePC). Nevertheless, DeePO is computationally more efficient than DeePC, as it is gradient-based and does not require solving optimization problems online.

Future work includes the extension of DeePO to achieve other control objectives (e.g., reference tracking) and to other types of systems (e.g., slowly time-varying systems).

APPENDIX I PROOF OF THEOREM 1

The state can be represented with system dynamics and history trajectories as

$$\begin{aligned} x_t &= A^n x_{t-n} + \mathcal{C}u_{t,n} + \mathcal{C}_w w_{t,n} \\ y_{t,n} &= \mathcal{O}x_{t-n} + \mathcal{T}u_{t,n} + \mathcal{T}_w w_{t,n} + v_{t,n}. \end{aligned} \quad (13)$$

Since \mathcal{O} has full column rank, it has a unique left pseudo inverse $\mathcal{O}^\dagger = (\mathcal{O}^\top \mathcal{O})^{-1} \mathcal{O}^\top$. Then, it follows immediately from (13) that

$$x_t = (\mathcal{C} - A^n \mathcal{O}^\dagger \mathcal{T}) u_{t,n} + A^n \mathcal{O}^\dagger y_{t,n} \\ + (\mathcal{C}_w - A^n \mathcal{O}^\dagger \mathcal{T}_w) w_{t,n} - A^n \mathcal{O}^\dagger v_{t,n},$$

and $y_t = Cx_t + v_t = Sz_t + d_t$. Thus, a non-minimal realization of (1) is given by (11).

The proof for controllability of (11) follows the same vein of that of the key reachability lemma in [30, Lemma 3.4.7]. Note that their relatively prime condition holds for the system (1) since the length of the past trajectory used to represent the state matches the system order n .

REFERENCES

- [1] F. Milano, F. Dörfler, G. Hug, D. J. Hill, and G. Verbič, “Foundations and challenges of low-inertia systems,” in *2018 Power Systems Computation Conference (PSCC)*, 2018, pp. 1–25.
- [2] L. Huang, H. Xin, Z. Wang, W. Huang, and K. Wang, “An adaptive phase-locked loop to improve stability of voltage source converters in weak grids,” in *2018 IEEE Power & Energy Society General Meeting (PESGM)*, 2018, pp. 1–5.
- [3] L. Huang, H. Xin, Z. Li, P. Ju, H. Yuan, Z. Lan, and Z. Wang, “Grid-synchronization stability analysis and loop shaping for pll-based power converters with different reactive power control,” *IEEE Trans. Smart Grid*, vol. 11, no. 1, pp. 501–516, 2019.
- [4] X. Wang, L. Harnefors, and F. Blaabjerg, “Unified impedance model of grid-connected voltage-source converters,” *IEEE Trans. Power Electronics*, vol. 33, no. 2, pp. 1775–1787, 2017.
- [5] Y. Cheng *et al.*, “Wind energy systems sub-synchronous oscillations: Events and modeling,” *IEEE Power & Energy Society: Piscataway, NJ, USA, Tech. Rep., PES-TR80*, 2020.
- [6] L. Harnefors, “Modeling of three-phase dynamic systems using complex transfer functions and transfer matrices,” *IEEE Transactions on Industrial Electronics*, vol. 54, no. 4, pp. 2239–2248, 2007.
- [7] M. Cespedes and J. Sun, “Impedance modeling and analysis of grid-connected voltage-source converters,” *IEEE Transactions on Power Electronics*, vol. 29, no. 3, pp. 1254–1261, 2013.
- [8] J. Zhou, P. Shi, D. Gan, Y. Xu, H. Xin, C. Jiang, H. Xie, and T. Wu, “Large-scale power system robust stability analysis based on value set approach,” *IEEE Transactions on Power Systems*, vol. 32, no. 5, pp. 4012–4023, 2017.
- [9] G. Weiss, Q.-C. Zhong, T. C. Green, and J. Liang, “ H_∞ repetitive control of DC-AC converters in microgrids,” *IEEE Transactions on Power Electronics*, vol. 19, no. 1, pp. 219–230, 2004.
- [10] F. Zhao, K. You, and T. Başar, “Global convergence of policy gradient primal-dual methods for risk-constrained LQRs,” *IEEE Transactions on Automatic Control*, vol. 68, no. 5, pp. 2934–2949, 2023.
- [11] F. Zhao, X. Fu, and K. You, “Convergence and sample complexity of policy gradient methods for stabilizing linear systems,” *IEEE Transactions on Automatic Control*, 2024.
- [12] J. Coulson, J. Lygeros, and F. Dörfler, “Data-enabled predictive control: In the shallows of the DeePC,” in *18th European Control Conference (ECC)*, 2019, pp. 307–312.
- [13] F. Dörfler, J. Coulson, and I. Markovskiy, “Bridging direct and indirect data-driven control formulations via regularizations and relaxations,” *IEEE Transactions on Automatic Control*, vol. 68, no. 2, pp. 883–897, 2023.
- [14] F. Dörfler, P. Tesi, and C. De Persis, “On the certainty-equivalence approach to direct data-driven LQR design,” *IEEE Transactions on Automatic Control*, vol. 68, no. 12, pp. 7989–7996, 2023.
- [15] A. Chiuso, M. Fabris, V. Breschi, and S. Formentin, “Harnessing the final control error for optimal data-driven predictive control,” *arXiv preprint arXiv:2312.14788*, 2023.
- [16] C. De Persis and P. Tesi, “Formulas for data-driven control: Stabilization, optimality, and robustness,” *IEEE Transactions on Automatic Control*, vol. 65, no. 3, pp. 909–924, 2019.
- [17] H. J. Van Waarde, J. Eising, H. L. Trentelman, and M. K. Camlibel, “Data informativity: a new perspective on data-driven analysis and control,” *IEEE Transactions on Automatic Control*, vol. 65, no. 11, pp. 4753–4768, 2020.
- [18] W. Liu, G. Wang, J. Sun, F. Bullo, and J. Chen, “Learning robust data-based lqg controllers from noisy data,” *IEEE Transactions on Automatic Control*, 2024.
- [19] S. Kang and K. You, “Minimum input design for direct data-driven property identification of unknown linear systems,” *Automatica*, vol. 156, p. 111130, 2023.
- [20] I. Markovskiy and F. Dörfler, “Behavioral systems theory in data-driven analysis, signal processing, and control,” *Annual Reviews in Control*, vol. 52, pp. 42–64, 2021.
- [21] I. Markovskiy, L. Huang, and F. Dörfler, “Data-driven control based on the behavioral approach: From theory to applications in power systems,” *IEEE Control Systems Magazine*, vol. 43, no. 5, pp. 28–68, 2023.
- [22] F. Dörfler, “Data-driven control: Part two of two: Hot take: Why not go with models?” *IEEE Control Systems Magazine*, vol. 43, no. 6, pp. 27–31, 2023.
- [23] F. Zhao, F. Dörfler, and K. You, “Data-enabled policy optimization for the linear quadratic regulator,” in *62nd IEEE Conference on Decision and Control (CDC)*, 2023, pp. 6160–6165.
- [24] F. Zhao, F. Dörfler, A. Chiuso, and K. You, “Data-enabled policy optimization for direct adaptive learning of the LQR,” *arXiv preprint arXiv:2401.14871*, 2024.
- [25] L. Huang, J. Coulson, J. Lygeros, and F. Dörfler, “Data-enabled predictive control for grid-connected power converters,” in *IEEE Conf. on Decision and Control*, 2019.
- [26] B. D. Anderson and J. B. Moore, *Optimal control: linear quadratic methods*. Courier Corporation, 2007.
- [27] B. Hu, K. Zhang, N. Li, M. Mesbahi, M. Fazel, and T. Başar, “Toward a theoretical foundation of policy optimization for learning control policies,” *Annual Review of Control, Robotics, and Autonomous Systems*, vol. 6, pp. 123–158, 2023.
- [28] J. C. Willems, P. Rapisarda, I. Markovskiy, and B. L. De Moor, “A note on persistency of excitation,” *Systems & Control Letters*, vol. 54, no. 4, pp. 325–329, 2005.
- [29] F. Zhao, X. Fu, and K. You, “Globally convergent policy gradient methods for linear quadratic control of partially observed systems,” *IFAC-PapersOnLine*, vol. 56, no. 2, pp. 5506–5511, 2023.
- [30] G. C. Goodwin and K. S. Sin, *Adaptive filtering prediction and control*. Courier Corporation, 2014.